

COVER PAGE

Document downloaded by @DAEL

Sun Nov 29 16:31:23 2026
For personal use

When automatic English translation is provided, only the original document is authentic.
The EAA cannot be held responsible of any translation error

Bibliographical reference

Sabine Absorption Coefficient Predictions Using Different Radiation Impedances of a Finite Absorber, Cheol-Ho Jeong, Acta Acustica **vol. 101** (Number 4), 2015, pp. 663-667

DOI
https://doi.org/10.3813/AAA.918861

ACTA ACUSTICA UNITED WITH ACUSTICA
Vol. 101 (2015) 663 – 667

DOI 10.3813/AAA.918861

Sabine Absorption Coefficient Predictions Using Different Radiation Impedances of a Finite Absorber

Cheol-Ho Jeong
Acoustic Technology, Department of Electrical Engineering, Technical University of Denmark, DK-2800, Kongens Lyngby, Denmark. chj@elektro.dtu.dk

PACS no. 43.55.Ev

1. Introduction

There are two ways of measuring the absorption properties of acoustic elements. The first one is the tube method [1], which assumes plane wave propagation at the normal direction to a test sample. This method has limitations when testing 3D objects, such as furniture, and only the normal incidence acoustic quantities are measured. The other method is the chamber method according to ISO 354 [2]. The Sabine absorption coefficient, α_{Sab}, is calculated via Sabine's formula based on the reverberation time measurements with and without an absorber specimen in a reverberation chamber [3].

The Sabine absorption coefficient has two main problems. First, it can exceed unity and is likely to be higher than the random incidence absorption coefficient [4]. Absorption coefficients higher than unity cannot be used in acoustics simulations, such as image source method, ray tracing, and finite and boundary element method, because no reflection model can deal with such values. A major reason for such high absorption values is known to be diffraction from the edge of a finite test sample [5, 6]. To account for the increase in the measured equivalent absorption coefficient, Thomasson derived a radiation impedance for finite surfaces [7, 8], simply referred to as the finite surface radiation impedance in what follows, which has been commonly used in calculation of sound absorption coefficient and transmission index [9, 10, 11, 12, 13, 14, 15, 16].

The second problem of the Sabine absorption coefficient is a poor inter-chamber reproducibility. Several absorption round-robin tests have shown that there are huge variations in the Sabine absorption coefficient measured in different chambers [4, 17, 18]. It is mainly because the reverberation chambers are non-diffuse in fundamentally different ways: different dimensions, different geometrical shapes, and different types and sizes of the diffusers used. Consequently, the angular distribution of the incident power onto the test sample differs largely [9, 10], which is directly related to the degree of directional diffusion in the chambers. Such a large room- to-room deviation can also be a problem for both acousticians and absorber manufacturers because the absorption coefficient measured in a specific chamber is likely to be biased by the test chamber.

The aim of this study is twofold. The first aim is to report the discrepancy between predictions of the Sabine absorption coefficient using the finite surface radiation impedance and round robin test data. The main reason for the discrepancy is that the fundamental assumptions behind the finite surface radiation impedance are violated in practical reverberation chamber measurements according to ISO 354. Since the absorption coefficient measured in a specific chamber cannot represent the average behavior of the test specimen, round robin test data are used as reference. The second aim is to clarify the grounds for the use of the complex conjugate of the radiation impedance in the author's previous publication [13], where the choice of the complex conjugate was neither clearly indicated nor explained.

Received 24 March 2015,
accepted 23 April 2015.

2. Method

2.1. Random incidence absorption coefficient

For plane wave incidence on an infinitely large surface, the oblique incidence absorption coefficient at an incidence angle θ_i, $\alpha_{\text{inf}}(\theta_i)$, is expressed as [19]

$$\alpha_{\text{inf}}(\theta_i) = \frac{\Re e\{Z_w\}}{\left(|Z_w|\cos\theta_i\right)^2 + 2\Re e\{Z_w\}\cos\theta_i + 1} = 1 - \left|\frac{\zeta - 1/\cos\theta_i}{\zeta + 1/\cos\theta_i}\right|^2. \quad (1)$$

Here, ζ is the surface impedance, Z_w, normalized by the characteristic impedance of air, $\rho_0 c_0$, ρ_0 being the air density and c_0 being the speed of sound in air.

The theoretical random incidence absorption coefficient is calculated by Paris' law [19] as

$$\alpha_{\text{rand}} = \int_0^{\pi/2} \alpha_{\text{inf}}(\theta_i)\sin(2\theta_i)\,\mathrm{d}\theta_i. \quad (2)$$

It is assumed that the intensity of the incident sound is uniformly distributed over all possible directions, and the phases of the waves incident on the absorber are randomly distributed [19]. This random incidence absorption coefficient should range between 0 and unity.

2.2. Prediction of Sabine absorption coefficient

Thomasson derived the radiation impedance for a finite absorber under the following assumptions [7]. He assumed a locally reacting absorber, which is flush with an acoustically rigid and infinitely large floor. Using a variational formulation, the pressure distribution over the absorber is found, from which the absorption coefficient is calculated [7],

$$\alpha_{\text{fin}}(\theta_i) = \frac{4\Re e\{\zeta\}}{\left|\zeta + Z_r(\theta_i)\right|^2}\frac{1}{\cos\theta_i}. \quad (3)$$

Here, $Z_r(\theta_i)$ is the averaged radiation impedance over azimuthal angles from 0 to 2π expressed as $Z_r(\theta_i) = \int_0^{2\pi} Z_r(\theta_i,\varphi)\,\mathrm{d}\varphi/2\pi$, φ is the azimuth angle, and $Z_r(\theta_i,\varphi)$ is the radiation impedance. Note that Equation (3) of [12] is incorrect and thus should be changed to Equation (3). Atalla *et al.* also ended up with the same oblique incidence absorption coefficient in Equation (3) [20]. Conversely, Equation (3) becomes Equation (1) by replacing Z_r by $1/\cos\theta_i$ for infinite surfaces. The radiation impedance for a finite surface was derived as follows (for more information, see Equation (A1) in [7] and Equation (18) in [8]),

$$Z_r(\theta_i,\varphi) = \frac{\mathrm{j}k}{S}\iint_{S_a}\iint_{S_a} G\mathrm{e}^{\mathrm{j}k\left[\mu_x(x_0-x)+\mu_y(y_0-y)\right]}\,\mathrm{d}x\,\mathrm{d}y\,\mathrm{d}x_0\,\mathrm{d}y_0, \quad (4)$$

where k is the wavenumber, $S = \iint_{S_a}\mathrm{d}x\,\mathrm{d}y$, $\mu_x = \sin\theta_i\cos\varphi$, $\mu_y = \sin\theta_i\sin\varphi$, $G = -1/(2\pi R)\exp(\mathrm{j}kR)$, and $R = [(x-x_0)^2+$

© S. Hirzel Verlag · EAA

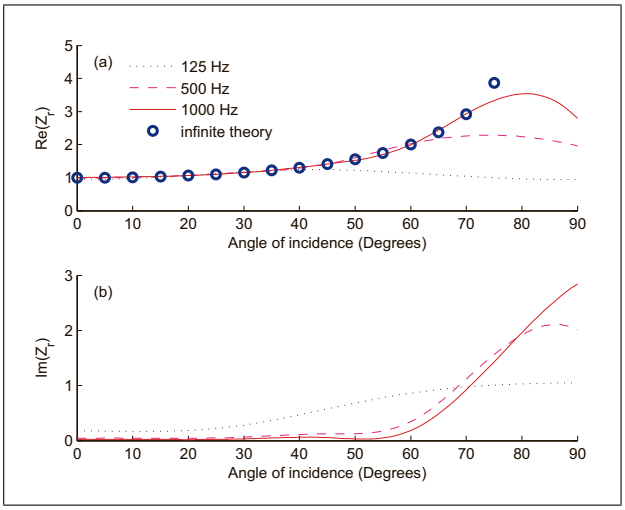


Figure 1. Radiation impedance of a finite absorber of 11 m^2 assuming exp(jωt). (a) Resistance, (b) reactance.

$(y - y_0)^2]^{1/2}$. Brunskog suggested another equation for effective calculation of $Z_r(\theta_i, \varphi)$ [14].

The finite surface radiation impedance at different frequencies for a sample size of 11 m^2 is displayed along with the infinite surface radiation impedance of $1/\cos\theta_i$ in Figure 1. Larger differences are found at near grazing incidence angles and low frequencies [7, 16]. The radiation impedances for finite surfaces agree well with those for infinitely large surfaces up to a certain angle. Since exp(−jωt) is assumed in Thomasson's original derivation [7], the radiation impedance has a negative reactance term in [7, 11, 12], whereas Davy *et al.* and Brunskog presented positive reactance values by using the opposite time conversion, exp(jωt) [14, 15]. Despite the opposite sign of the reactance, the results are identical. One noticeable difference between finite and infinite absorbers is that the radiation impedance for a finite surface is a complex quantity, whereas that for an infinite surface, $1/\cos\theta_i$, is purely real.

When acoustic excitation is exerted on a finite absorber, it vibrates and radiates sound into air. The radiation impedance is the impedance of the surface that radiates sound in the surrounding medium. The imaginary part of the finite surface radiation impedance in Figure 1 indicates mass loading. This mass loading is mainly caused by the discontinuity in the surface impedance between the test absorber and infinite rigid baffle since the radiation impedance for an infinite absorber without a baffle is purely real. In practical measurements, the baffle that is represented by the floor of the test chamber is indeed finite, so this mass loading effect is likely to be weaker than theoretically derived in Equation (4).

By applying Paris's law to Equation (3), the statistical absorption coefficient considering the size effect is expressed as [7, 9, 10, 12]

$$\alpha_{\text{size,org}} = 2\int_0^{\pi/2} \frac{4\Re e\{\zeta\}}{\left|\zeta + Z_r(\theta_i)\right|^2} \sin\theta_i \, \mathrm{d}\theta_i. \tag{5}$$

Two alternative uses of the finite surface radiation impedance are tested in this study. The first alternative is to approximate the finite surface radiation impedance to the real part of the original radiation impedance. Therefore, the predicted absorption coefficient is given by

$$\alpha_{\text{size,real}} = 2\int_0^{\pi/2} \frac{4\Re e\{\zeta\}}{\left|\zeta + \Re e\left\{Z_r(\theta_i)\right\}\right|^2} \sin\theta_i \, \mathrm{d}\theta_i. \tag{6}$$

Note that the resistance for the finite sample agrees well with the infinite panel theory up to 40° at 125 Hz, 60° at 500 Hz, and 75° at 1 kHz in Figure 1a. Therefore, the use of $\Re e\{Z_r\}$ in Equation (6) can be interpreted approximately as an angle truncation in Paris' law using the infinite surface radiation impedance of $1/\cos\theta_i$ as

$$\alpha_{\text{size,real}} \approx 2\int_0^{\theta_{i,\text{trun}}} \frac{4\Re e\{\zeta\}}{\left|\zeta + 1/\cos(\theta_i)\right|^2} \sin\theta_i \, \mathrm{d}\theta_i. \tag{7}$$

Here, $\theta_{i,\text{trun}}$ is the truncation angle, which varies with the frequency and sample size, for example, 75° for 1 kHz with a sample size of 11 m^2 as shown in Figure 1a.

The other alternative is to use the complex conjugate of the finite surface radiation impedance, which is rather empirically chosen. This inversion of the sign of the reactance means that there is a spring effect rather than mass loading, which has not been theoretically proven yet. In order to theoretically tackle this problem, one needs to combine the irregularity in the surface admittance and surface roughness together, as some initial derivations were done by Morse and Ingard in Section 8.3 of [21], since actual measurements fulfil neither the infinite baffle nor the flush mounting condition. However, this is beyond the scope of this study because the main purpose of this paper is to report the discrepancy between absorption predictions and round robin test data in violation of the original assumptions. In [13], this complex conjugate was used to inversely identify the flow resistivity of a test specimen, which gave a satisfactory result. Equation (1) in [13] should be corrected to

$$\alpha_{\text{size,conj}} = 2\int_0^{\pi/2} \frac{4\Re e\{\zeta\}}{\left|\zeta + Z_r^*(\theta_i)\right|^2} \sin\theta_i \, \mathrm{d}\theta_i. \tag{8}$$

2.3. Error measures

Three error measures are proposed. First, e_1 is the average absolute difference between the simulation and measurement at frequencies lower than and equal to 500 Hz. Second, e_2 is the average absolute difference between the prediction and measurement at frequencies higher than 500 Hz. The choice of 500 Hz is ascribed to the fact that it is the closest octave band center frequency to the Schroder frequency of 400 Hz for a typical reverberation chamber, assuming its empty condition reverberation time as 10 s and its volume as 250 m^3. Below the Schroeder frequency, larger measurement uncertainties are expected. The third measure is a shape similarity using Pearson's linear correlation coefficient [22] between the measured and predicted absorption coefficients.

2.4. Three round robin tests

In Kosten's round robin test, the test specimen was a 5 cm thick rockwool with a density of 100 kg/m^3 [4]. The surface impedance of the test material can be found in Thomasson's report [7]. Three different surface areas of 4 m^2, 8 m^2, and 12 m^2 were tested and averaged over 19 different reverberation chambers in the world. The actual dimensions and aspect ratios of the test samples differed, e.g., the surface area varied from 7.5 m^2 to 8.25 m^2 in different chambers for the 8 m^2 sample.

Vercammen conducted a round robin test with a rigidly-backed mineral wool (Rockwool, type 211) absorber of a thickness of 10 cm, which is directly mounted on the floor of 13 European chambers [17]. The density of the specimen was 44 kg/m^3. The flow resistivity value was measured to be 19.8 kNs/m^4. The sample size was 11.8 m^2.

Nolan *et al.* measured the absorption coefficient of a 10 cm glass wool (Saint-Gobain Ecophon, Industry Modus) backed by an air cavity of 10 cm in five European chambers [18]. Additionally, two more measurements in KU Leuven and RWTH Aachen chambers have been included, ending up with a total of 7 chamber measurements. The total construction height, d_{tot}, as shown in Figure 4, was 20 cm and the flow resistivity of the absorber was measured to be 12.9 kNs/m^4. The sample size was 11.8 m^2.

For the latter two round robin tests by Vercammen and Nolan *et al.*, the normal incidence surface impedance is not directly given. Therefore, Miki's impedance model was used to calculate the surface impedance of the test absorbers, which reads [23]

$$Z_c = \rho_0 c_0 \left(1 + 0.070\left(\frac{f}{\sigma}\right)^{-0.632} - \mathrm{j}0.107\left(\frac{f}{\sigma}\right)^{-0.632}\right), \quad (9a)$$

$$k_t = \frac{\omega}{c_0}\left(1 + 0.109\left(\frac{f}{\sigma}\right)^{-0.618} - \mathrm{j}0.160\left(\frac{f}{\sigma}\right)^{-0.618}\right). \quad (9b)$$

Based on Z_c and k_t, the surface impedance can be computed. For an absorber having a thickness d, which has a backing surface impedance of $Z|_{x=d}$, the surface impedance in front of the total construction at $x = 0$ for a plane wave incident at an angle θ_i is [24]

$$Z_w(f,\theta_i) = \frac{Z_c k_0}{k_x}\left(\frac{-\mathrm{j}Z\big|_{x=d}\cot\left(k_x d\right) + Z_c\frac{k_0}{k_x}}{Z\big|_{x=d} - \mathrm{j}Z_c\frac{k_0}{k_x}\cot\left(k_x d\right)}\right), \quad (10)$$

where k_x is the normal component of k_t ($k_x = \sqrt{k_t^2 - k_0^2\sin^2\theta_i}$), k_0 is the wave number in air, and j is the imaginary unit. If the backing surface is acoustically rigid ($Z|_{x=d} = \infty$), Equation (10) is simplified to $Z_w(f,\theta_i) = -\mathrm{j}(k_0/k_x)\cot(k_x d)$. For absorbers backed by an air cavity, $Z|_{x=d}(f,\theta_i)$ can be substituted by $-\mathrm{j}(\rho_0 c_0 k_0/k_x)\cot(k_0 d_0\cos\theta_i)$, where d_0 is the air cavity depth.

3. Comparison between round robin data and predictions

In practice, all the absorption measurements in reverberation chambers cannot satisfy the underlying assumptions of the finite surface radiation impedance. First, the reverberation chamber floors are finite, thus cannot satisfy the infinite baffle condition. Second, the test absorbers are not flush-mounted. Therefore, two comparisons are made: different area ratios between the test sample and the floor, and different heights of the absorber constructions.

3.1. Area ratio between the specimen and chamber floor

In Kosten's round robin test, three absorber sizes were tested as 4 m^2, 8 m^2, and 12 m^2. Assuming that they were square samples, the characteristic lengths, $e = \sqrt{s}$, were 2 m, 2.8 m, and 3.5 m, respectively. In most reverberation chambers, the floor area is no larger than 40 m^2. Therefore, the area ratios between the sample and floor are approximately 0.1, 0.2, and 0.3, respectively. Figure 2 shows the averaged Sabine absorption coefficient over the 19 chambers and the absorption predictions by Equations (5), (6), and (8), each using the original radiation impedance, its real part, and its complex conjugate, respectively. Note Kosten did not provide the standard deviation of the Sabine absorption coefficient. Figure 3 shows the error measures for different radiation impedances and different area ratios. For this 5 cm absorber specimen, the original radiation impedance works well except for the largest sample size; for the largest sample, the use of $\Re e\{Z_r\}$ performs best in terms of all the error measures. The complex conjugate Z_r^* performs worst, but still the correlation coefficient is reasonably higher than 0.95 for all sample sizes.

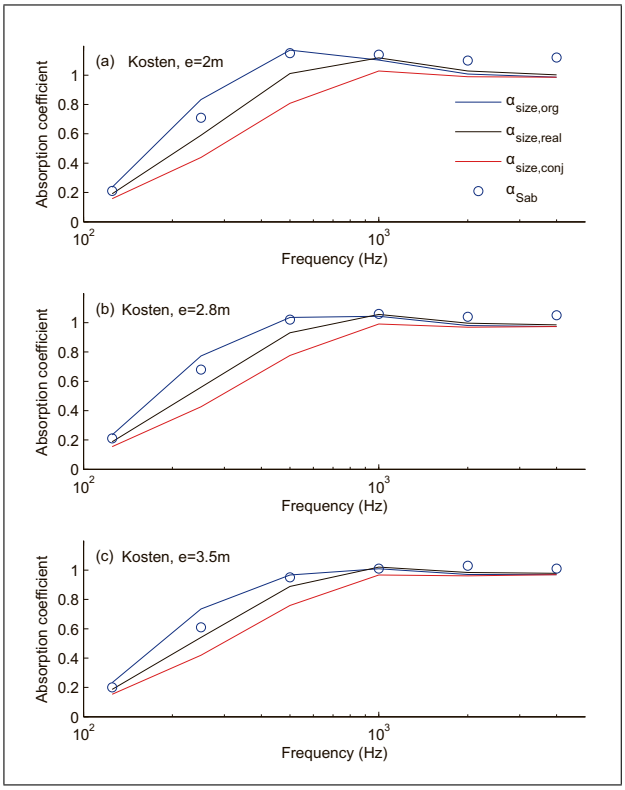


Figure 2. Comparison of the Sabine absorption coefficient between Kosten's measurement and predictions by changing the sample size. (a) $e = 2$ m, (b) $e = 2.8$ m, (c) $e = 3.5$ m.

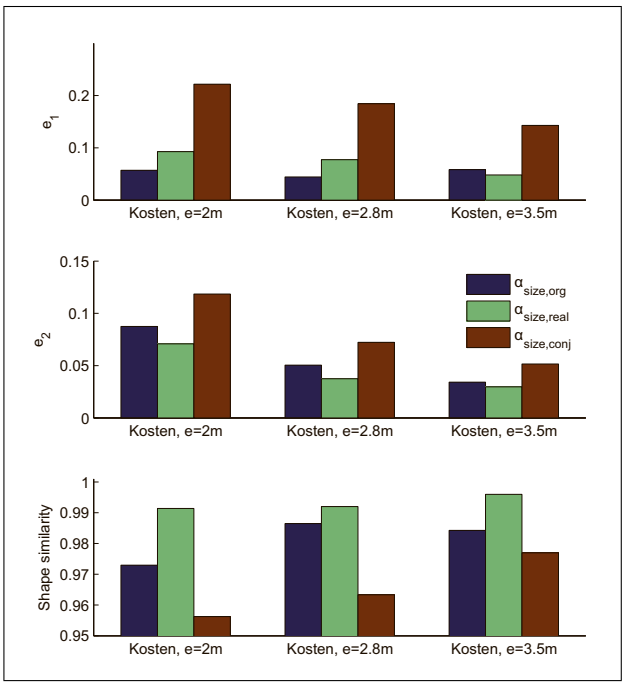


Figure 3. Error measures for different sample sizes. (a) e_1, (b) e_2, (c) shape similarity.

3.2. Thickness of the total absorber construction

Thomasson originally assumed a flush mounting on an infinite rigid baffle. In practice, the test absorber is located on the floor of the test reverberation chamber. In this sense, the thicker the absorber configuration, the more violated the flush mounting assumption is. The three round robin absorption data are compared for a similar size: around 12 m^2 for Kosten's sample and 11.8 m^2 for the other two. The thickness of the absorber construction is 5 cm for Kosten's data, 10 cm for Vercammen' data, and 20 cm for Nolan *et al.*'s data. In Figure 4, the average Sabine absorption coefficient and the predicted absorption coefficients are compared. Note the error bar indicates the standard deviation in Figures 4b and 4c. A gradual increase in the discrepancy toward the low frequency using Z_r and $\Re e\{Z_r\}$ is observed, as d_{tot} increases. The low frequency error gets significantly reduced using Z_r^*, as the thickness of the absorber construction increases. The high frequency error barely depends on the radiation impedance model, which indicates that the violation of the assumptions influences the radiation impedances more at lower frequencies.

The error measures are presented in Figure 5, where the low frequency error depends critically on the radiation impedance used. For the thinnest sample by Kosten, $\Re e\{Z_r\}$ works best. For the 10 cm sample by Vercammen, the accuracy of the prediction is degraded enormously with the original Z_r, and the least errors are found with $\Re e\{Z_r\}$ and Z_r^* in terms of e_2 and the shape similarity, respectively. The original Z_r performs the worst in terms of all the error measures. For the thickest sample by Nolan *et al.*, the improvement by using Z_r^* is substantial: the best shape similarity and the smallest low/high frequency error. The low frequency error using Z_r^* is 0.06, whereas those using $\Re e\{Z_r\}$ and Z_r are 0.23 and 0.40, respectively. In all round robin measurements, the correlation coefficient using Z_r^* is quite high, as all the values are larger than 0.98, whereas that using Z_r drops from 0.98 for the thinnest sample to 0.07 for the thickest sample.

4. Additional remarks

When actual measurement conditions are similar to the underlying assumptions of the finite surface radiation impedance, i.e., thin and small specimens, the original radiation impedance works best as shown in Figures 2 and 3. As the size becomes larger, the alternative radiation impedances start to perform better. ISO 354 recommends a specimen size between 10 m^2 and 12 m^2, according to which the largest sample size ($e = 3.5$ m) is only qualified. This means that the use of the original radiation impedance for most standardized tests degrades the accuracy of the absorption predictions. Moreover, as the absorber thickness increases, more deviations are found in Figures 4 and 5, which indicates that the flush mounting condition might be a central assumption for the deriving the radiation impedance.

Only a limited number of round robin absorption datasets are compared in this study since the Sabine absorption coefficient varies largely with the test chamber. More concrete conclusions could have been drawn with more round robin absorption results. The author found surface impedance values and Sabine absorption coefficients named $\alpha_{\text{A.M.A}}$ (A.M.A stands for Acoustic Materials Association) for materials thinner than or close to one inch in the old literature [25, 26, 27], but Hunt also specifically remarked that $\alpha_{\text{A.M.A}}$ is one of the many possible chamber coefficients [25, 28]. The original radiation impedance applied to such thin materials, e.g., Temcoustic 0.5", Acoustex, 0.9", Permacoustic, 1", and Celotex C4, 1.25", predicts $\alpha_{\text{A.M.A}}$ quite accurately; the average error is 0.06 for Temcoustic, 0.1 for Acoustex, 0.07 for Permacoustic, and 0.05 for Celotex C4, assuming their sample sizes as 6.68 m^2 (72 ft^2), which is guessed from the description of the typical sample size tested in the Riverbank chamber, where $\alpha_{\text{A.M.A}}$ was measured [29]. Consequently, the original finite surface radiation impedance in Equation (4) works well for relatively thin absorbers, as it approximately replicates the flush mounting condition.

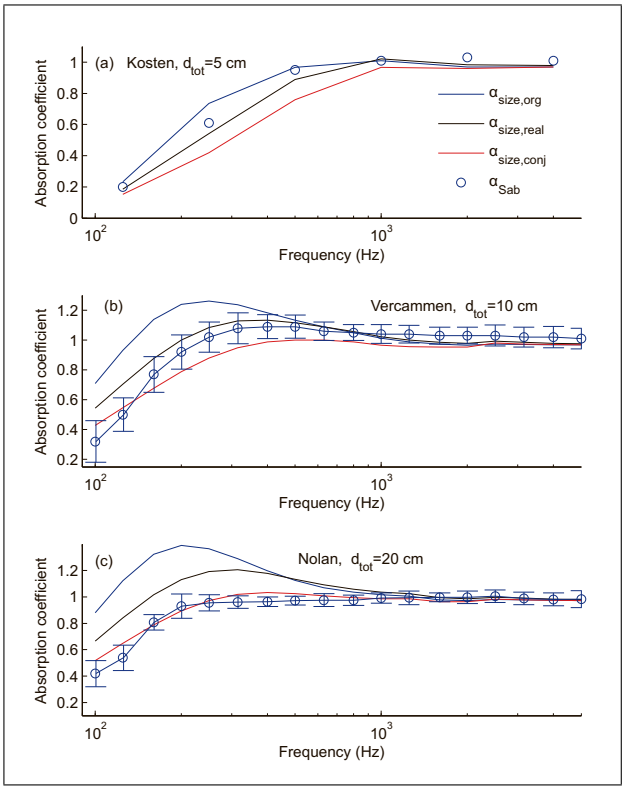


Figure 4. Comparison of the Sabine absorption coefficient between round robin measurements and predictions by changing the thickness of the absorber configuration. (a) $d_{\text{tot}} = 5$ cm, (b) $d_{\text{tot}} = 10$ cm, (c) $d_{\text{tot}} = 20$ cm.

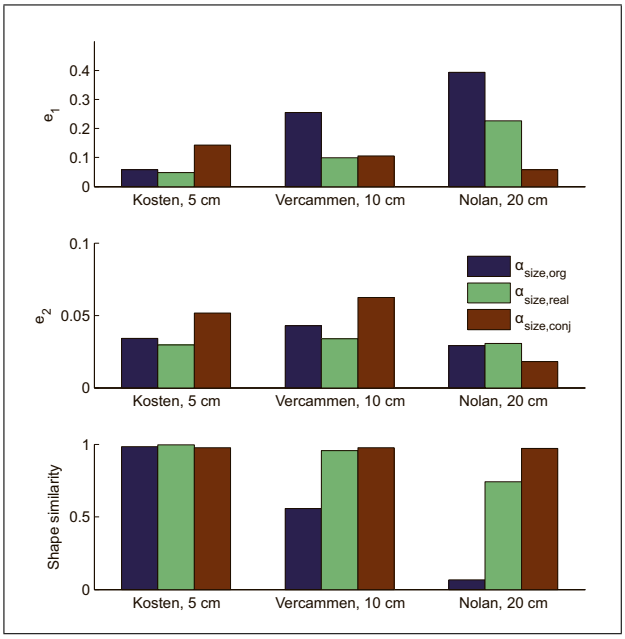


Figure 5. Error measures for different thickness conditions. (a) e_1, (b) e_2, (c) shape similarity.

5. Conclusions

This study is concerned with how departures from the underlying assumptions behind the finite surface radiation impedance affect the absorption predictions as compared to three round robin absorption data. Two comparisons between three absorption prediction models and round robin data are made by varying the sample size and the absorber thickness. The larger the sample size, the larger the discrepancy between the measurements and predictions using the finite surface radiation impedance. The thicker the absorber configuration is, the larger the discrepancy. It was found that the use of Thomasson's radiation impedance is more sensitive to the test absorber thickness and sample size tested. Two alternative radiation impedances, the real part and complex conjugate of the finite surface radiation impedance, perform better than Thomasson's radiation impedance in most practical measurements, and the reason for this should be further investigated theoretically.

References

[1] ISO 10534-2:1998: Acoustics - Determination of sound absorption coefficient and impedance in impedance tubes - Part 2: Transfer function method. 1998.

[2] ISO 354:2003: Acoustics - Measurement of sound absorption in a reverberation room. 2003.

[3] C. Morfey: Dictionary of acoustics. Academic Press, London, 2001.

[4] C. W. Kosten: International comparison measurement in the reverberation room. Acustica **10** (1960) 400–411.

[5] T. T. Wolde: Measurements on the edge-effect in reverberation rooms. Acustica **18** (1967) 207–212.

[6] W. Kuhl: Der Einfluss der Kanten auf die Schall-absorption poröser Materialien. Acustica **10** (1960) 264.

[7] S.-I. Thomasson: Theory and experiments on the sound absorption as function of the area. Report TRITA-TAK 8201, Royal Institute of Technology, Sweden, 1982.

[8] S.-I. Thomasson: On the absorption coefficient. Acustica **44** (1980) 265–273.

[9] C.-H. Jeong: A correction of random incidence absorption coefficients for the angular distribution of acoustic energy under measurement conditions. J. Acoust. Soc. Am. **125** (2009) 2064–2071.

[10] C.-H. Jeong: Non-uniform sound intensity distributions when measuring absorption coefficients in reverberation chambers using a phased beam tracing. J. Acoust. Soc. Am. **127** (2010) 3560–3568.

[11] C.-H. Jeong: Improved low frequency responses by considering finiteness of room boundary surfaces. Acta Acustica United with Acustica **99** (2013) 545–556.

[12] C.-H. Jeong: Converting Sabine absorption coefficients to random incidence absorption coefficients. J. Acoust. Soc. Am. **133** (2013) 3951–3962.

[13] C.-H. Jeong, J.-H. Chang: Reproducibility of the random incidence absorption coefficient converted from the Sabine absorption coefficient. Acta Acustica united with Acustica **101** (2015) 99–112.

[14] J. Brunskog: The forced sound transmission of finite single leaf walls using a variational technique. J. Acoust. Soc. Am. **132** (2012) 1482–1493.

[15] J. L. Davy, D. J. Larner, R. R. Wareing, J. R. Pearse: The average specific forced radiation wave impedance of a finite rectangular panel. J. Acoust. Soc. Am. **136** (2014) 525–536.

[16] J. H. Rindel: Modeling the angle-dependent pressure reflection factor. Applied Acoustics **38** (1993) 223–234.

[17] M. Vercammen: Improving the accuracy of sound absorption measurement according to ISO 354. Proceedings of the International Symposium on Room Acoustics, Melbourne, Australia, 2010.

[18] M. Nolan, M. Vercammen, C.-H. Jeong, J. Brunskog: The use of a reference absorber for absorption measurements in a reverberation chamber. Proceedings of Forum Acusticum 2014, Krakow, Poland, 2014.

[19] H. Kuttruff: Room acoustics. Spon Press, London, 2009.

[20] N. Atalla, F. Sgard, C. K. Amedin: On the modeling of sound radiation from poroelastic materials. J. Acoust. Soc. Am. **120** (2006) 1990–1995.

[21] P. M. Morse, K. U. Ingard: Theoretical acoustics. McGraw-Hill, New York, 1968.

[22] J. S. Bendat, A. G. Piersol: Random data: Analysis and measurement procedures. John Wiley & Sons, New York, 2000.

[23] Y. Miki: Acoustical properties of porous materials - modifications of Delany-Bazley models. J. Acoust. Soc. Jp. **11** (1990) 19–28.

[24] J.-F. Allard: Propagation of sound in porous media: Modelling sound absorbing materials. Elsevier Applied Science, London, 1993.

[25] P. M. Morse, R. H. Bolt, R. L. Brown: Acoustic impedance and sound absorption. J. Acoust. Soc. Am. **12** (1940) 217–227.

[26] A. London: The determination of reverberant sound absorption coefficients from acoustic impedance measurements. J. Acoust. Soc. Am. **22** (1950) 263–269.

[27] B. S. Atal: A semi-empirical method of calculating reverberation chamber coefficients from acoustic impedance value. Acustica **9** (1959) 27–30.

[28] F. V. Hunt: The absorption coefficient problem. J. Acoust. Soc. Am. **11** (1939) 38–40.

[29] P. E. Sabine: Measurement of sound absorption coefficients from the viewpoint of the testing laboratory. J. Acoust. Soc. Am. **11** (1939) 41–44.